Adsorption (2006) 12:423–434
DOI 10.1007/s10450-006-0570-0

Ortho-selectivity in aluminophosphate molecular sieves: A molecular simulation study

S. Mardônio P. Lucena · Célio L. Cavalcante Jr · João A. F. R. Pereira

Abstract Monte Carlo adsorption simulations of xylenes have been performed in aluminophosphate molecular sieve structures. A new force field fitted for *o*-xylene in $AlPO_4$-5 was used. It is shown that force fields have good transferability among the aluminophosphate sieves series and the new force field adequately describes the experimentally observed adsorption isotherms for xylene/$AlPO_4$-5. A previous investigation of adsorption isotherms and structural analysis has been extended to $AlPO_4$-8 and VPI-5 sieves. In $AlPO_4$-8, like in $AlPO_4$-5, the variations in the channels diameters and the corresponding interaction energy of the molecule-crystal lattice drive all molecular positioning. In VPI-5, the modulation between wide and narrow regions becomes negligible due to the larger pore diameter, so no ortho-selectivity was observed. The simulations confirm the ortho-selectivity mechanism proposed to aluminophosphates.

Keywords Aluminophosphates · Adsorption · Xylenes · Molecular simulation

S. M. P. Lucena · C. L. Cavalcante Jr (✉)
Universidade Federal do Ceará, Dept. Eng. Química, Grupo de Pesquisas em Separações por Adsorção, Campus do Pici, Bl. 709, 60455-760, Fortaleza, CE, Brazil
e-mail: celio@gpsa.ufc.br

J. A. F. R. Pereira
Universidade Estadual de Campinas, Faculdade de Engenharia Química, Campinas, SP Brazil

1 Introduction

The present study is related to the xylenes adsorption simulation in aluminophosphates. The aluminophosphates represent a series of molecular sieves first synthesized by Wilson et al. (1982) in the decade of 80. Most of the representatives of this series present unidimensional channels and a neutral framework. Some macroscopic measurements like Infra-Red (Barthomeuf and Mallmann, 1990), thermodynamic properties (Eder and Lercher, 1996; Jänchen et al., 1996) and diffusion coefficient measurements (Chiang et al., 1991; Cavalcante et al., 2000) have been carried out on aromatic molecules adsorbed in aluminophosphate, in order to understand their sorption and diffusion properties. Some of these studies (Barthomeuf and Mallmann, 1990; Chiang et al., 1991) were performed to investigate the ortho-selectivity behavior in aluminophosphates. Unlike silicalite that has *p*-xylene selectivity and NaY that has *m*-xylene selectivity, $AlPO_4$-5 has shown a surprising *o*-xylene selectivity.

There have been reports on molecular simulation of the adsorption of xylenes in silicalite (Snurr et al., 1993a,b) and in NaY (Lachet et al., 1998, 1999). Recently, we have reported preliminary studies on the adsorption of xylenes in aluminophosphates (Lucena et al., 2006). Using a simplified force field, it was observed that the channels modulation of the aluminophosphates and the corresponding interaction of the xylenes with the lattice drive all molecular

positioning which results in the ortho-selectivity behavior of the $AlPO_4$-5. Despite a good agreement in the *m*- and *p*-xylene isotherms for $AlPO_4$-5 and qualitative agreement in the ortho-selectivity, simulated adsorption heat values were much larger than the experimental values. Also only a fair agreement with experimental *o*-xylene isotherms was found for $AlPO_4$-5.

To resolve these discrepancies a new force field fitted to aluminophosphates was developed. To our knowledge no force field adjusted for xylenes in aluminophosphates has been proposed to this date. With the objective of evaluating the transferability of force fields among aluminophosphates we performed low loading adsorption heat comparative studies. Argon, ethane and benzene and the sieve series $AlPO_4$-5, $AlPO_4$-8, $AlPO_4$-11 and VPI-5 were checked using three other force fields. Pure-component adsorption isotherms for *o*-xylene and *p*-xylene in $AlPO_4$-5 were predicted again and compared with previously reported experimental data.

With the satisfactory results of the adsorption heats and isotherms we extended the xylenes ortho-selectivity study predicting equilibrium isotherms and adsorption heats at different loadings. Furthermore we present a structural analysis for the sieves VPI-5 and $AlPO_4$-8.

2 Simulation model

2.1 Structural details

The xylenes molecular structures were obtained through optimization based in intermolecular potentials of the force field CFF (Sun et al., 1994). The molecules were considered planar and rigid.

The aluminophosphate $AlPO_4$-5 crystallizes in the space group P6/mcc ($a = 13.8$ Å and $c = 8.45$ Å) with 72 atoms/unitary cell (Bennet et al., 1983). It forms one-dimensional pores with free diameter of 7.3 Å parallel to the crystallographic *c* direction (AFI structural network—hexagonal). $AlPO_4$-11 crystallizes in the space group Imma ($a = 13.534$ Å, $b = 18.482$ Å, $c = 8.370$ Å) with 120 atoms/unitary cell (Bennet et al., 1987) and one-dimensional pores with free diameter of 6.5×4.0 Å parallel to the crystallographic *c* direction (AEL structural network—orthorhombic).

VPI-5 crystallizes in a hexagonal space group $P6_3cm$ ($a = 19.0$ Å and $c = 8.11$ Å) with 108 atoms/unit cell (McCusker et al., 1991) and one-dimensional pores with free diameter of 12.7 Å (VFI structural network—hexagonal). $AlPO_4$-8 crystallizes in the space group Cmcm ($a = 32.8$ Å, $b = 14.4$ Å and $c = 8.4$ Å) with 216 atoms/unit cell (Dessau et al., 1990) and one-dimensional pores with free diameter of 8.35 Å (AET structural network -orthorhombic).

In all four aluminophosphates, the channels do not have uniform diameters. They exhibit modulation of diameter along the *c* axis, leading to alternate wide and narrow cross-sections. The narrow region is the oxygen ring (windows) and the wide region corresponds to the areas of connections between two oxygen windows (see Fig. 1).

$AlPO_4$-5 has narrow windows with 12 oxygen atoms with diameter of 9.96 Å and wide regions (connecting two consecutive windows) with diameter of 11.20 Å (Fig. 1(A)). $AlPO_4$-11 has windows with 10 oxygen atoms with diameters of 9.31×7.06 Å and wide regions with diameters of 10.40×7.80 Å. VPI-5 and $AlPO_4$-8 have windows with 14 and 18 oxygen atoms and with diameters of 15.0 Å and 10.6 Å respectively (Fig. 1(B) and 1(C)). The VPI-5 and $AlPO_4$-8 wide regions have diameters of 16.70 and 12.3 Å, respectively.

2.2 Interaction potentials

2.2.1 Sorbate-sorbate interaction

Xylene molecules were treated atom by atom (AA model) and the xylene-xylene interactions were modeled with a Lennard-Jones (LJ) potential.

$$U_{ij} = 4\varepsilon_{ij}\left\{\left(\frac{\sigma_{ij}}{r_{ij}}\right)^{12} - \left(\frac{\sigma_{ij}}{r_{ij}}\right)^{6}\right\} \quad (1)$$

The interaction parameters $\boldsymbol{\varepsilon_{ij}}$ and $\boldsymbol{\sigma_{ij}}$ were taken from Jorgensen et al. (1993) who developed an OPLS potential for toluene and other substituted benzenes. They used an atom-atom model for the substituted benzenes except methyl groups that are treated as united atoms centered on the carbon. With the objective of adequately reproducing the system geometry, we changed the methyl united atom model for an atom-atom model. Then carbons in the methyl groups are treated by the force field as aromatic ring carbon atoms. From our previous study (Lucena et al., 2006) it was observed that sorbate-sorbate interactions had only a minor effect

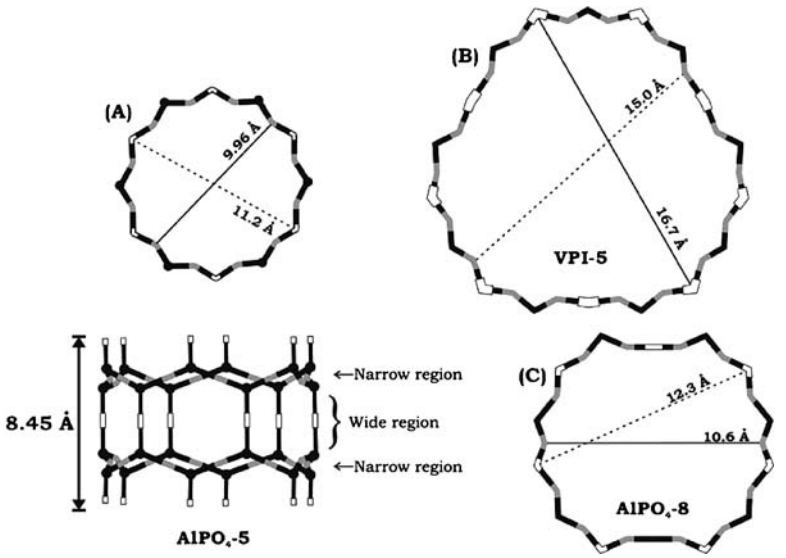

Fig. 1 Cross-sectional and vertical view of the channels of $AlPO_4$-5 (A) and cross-sectional views of VPI-5 (B) and $AlPO_4$-8 (C). (A) There are two diameters in the cross-sectional view, the narrow (9.96 Å) and the broad (11.20 Å). In the vertical view we can see the different regions indicated along the channel. The wide and narrow dimensions of the VPI-5 and $AlPO_4$-8 are shown in (B) and (C). The others vertical views (not shown) are very similar to the $AlPO_4$-5 view. (Diameters are taken between oxygen atoms of the narrow and wide regions. Aluminum and phosphorus atoms: black balls; Oxygen atoms in the windows: gray bars; Oxygen atoms in the wide regions: white bars. Cross-sectional views represent one wide and one narrow plane)

in the system behavior, thus the Coulomb interactions between different xylene molecules were not considered for this study. The parameters of this potential are listed in Table 1. The cross terms were obtained using arithmetic and geometric combination rules, as previously done by other authors (Clark and Snurr, 1999; Lachet et al., 1999; Frankel and Smith, 2002).

2.2.2 *Sorbate-aluminophosphate interaction*

In these systems, xylenes were assumed to interact only with the oxygen atoms of the molecular sieve framework. The dispersion-repulsion forces between xylene-aluminophosphates were modeled using Lennard-Jones potentials. We took LJ potentials between C and H and the oxygen atoms from Bhide and Yashonath (2000). We have adjusted the LJ parameters of the carbon in the methyl group so that the xylene-aluminophosphate interaction energy is close to the low loading adsorption heat value observed experimentally for *o*-xylene in $AlPO_4$-5 (Chiang et al., 1991). The values for these parameters can be seen in Table 1.

Table 1 LJ dispersion-repulsion parameters used in the calculations of xylene-xylene and xylene-aluminophosphates interactions (C3 is the carbon in the methyl group)

	C[a]	H[a]	C—O[b]	H—O[b]	C3—O[c]
σ (Å)	3.55	2.42	2.99	2.71	3.02
ε (kcal mol^{-1})	0.07	0.03	0.254	0.068	0.185

[a]From Jorgensen et al. (1993).
[b]From Bhide and Yashonath (2000).
[c]This study.

The interactions between Al and P atoms were ignored as previously done by other authors (Kiselev et al., 1985). No Coulomb interactions have been included between the xylenes and aluminophosphates. This can be justified because in neutral zeolitic structures, such as silicalite, the contribution of the electrostatic forces in high occupancy aromatic adsorption is only about 5–14% of the total value of the adsorption heat (Clark and Snurr, 1999).

2.3 Computational details

The calculations of adsorption heats and isotherms were performed in a simulation cell containing 27 unitary cells ($3 \times 3 \times 3$) for $AlPO_4$-5, $AlPO_4$-11 and VPI-5. For $AlPO_4$-8 the calculation of adsorption isotherms used a simulation cell containing 18 unitary cells ($2 \times 3 \times 3$). The GCMC technique was used in the adsorption isotherm simulations (Frenkel

and Smit, 2002). The algorithm allows displacements (translations and rotations), creations, and destructions. These simulations consisted of evaluating the average number of adsorbate molecules for which the chemical potential equals those of the bulk phase for a given pressure and temperature.

In the low loading adsorption heat calculations we used a canonical ensemble Monte Carlo algorithm (fixed loading) with only four xylene molecules in the simulation cell. The simulations were started by choosing the initial coordinates of the sorbate molecule, and then the algorithm allows translations and rotations of the molecules until the equilibrium is reached.

The simulations have been performed in a SGI Onyx2 station using Cerius2 software suite (Sorption, 2001). Between 1 and 4×10^6 Monte Carlo steps were performed in order to calculate mean values. The potentials cut-off distance was 12 Å, which is of the same order of magnitude of previous studies in similar systems (McCullen et al., 1993; Snurr et al., 1993a,b). The MC algorithms used a bad contact rejection factor (low cutoff) of 0.4 Å. Each run lasted from three to fourteen hours of computing time depending on the simulated system.

3 Results and discussion

3.1 Force field transferability in aluminophosphates

We only have a small number of available experimental data of xylenes adsorption in aluminophosphates. So, based in those data, we planned to use existing available force fields to check the effectiveness of the transferability among the aluminophosphate sieves. As we know, each force field is adjusted for a particular sorbate-molecular sieve system and then extended to other series members. If we find a good transferability pattern among the aluminophosphate sieves for other force fields, we can expect the same behavior for our new force field (fitted only to *o*-xylene/ $AlPO_4$-5 system).

There are no adsorption experimental data for xylenes in $AlPO_4$-8 and VPI-5. We only have xylenes experimental data available for $AlPO_4$-5 and $AlPO_4$-11 (Chiang et al., 1991; Cavalcante et al., 2000). For VPI-5, experimental data can be found only for low loading adsorption heats of benzene (Jänchen et al., 1996; McCullen et al., 1993). For $AlPO_4$-8, there are no aromatic compounds data available. Also, a reliable experimental series of low loading adsorption heats can only be found for the molecules of argon, ethane and benzene in $AlPO_4$-5, $AlPO_4$-11 and VPI-5 (McCullen et al., 1993; Reichert et al., 1994; Jänchen et al., 1996).

In the comparative study, besides our force field, force fields developed by Cracknell and Gubbins (1993) for argon, Bhide and Yashonath (2002) for ethane, and Bhide and Yashonath (2000) for benzene were used (seeTable 2). We have correlated the heat of adsorption with the framework density (FD) expressed in number of T-atoms per nm^3 (T/1000 $Å^3$) as previously reported by Jänchen et al. (1996). Table 3 presents the results of this comparative study. We observe that the series of values for argon is perfectly transferable. All the simulated values are approximately 0.25 kcal/mol larger than the experimental ones. For ethane we have an excellent agreement between the results. For benzene, the simulated values are around 2.5 kcal/mol larger than the experimental values for VPI-5 and $AlPO_4$-5, showing good transferability.

Table 2 Force field parameters used in the comparative study (Buckingham parameters A, B and C from Demontis et al., 1989)

	Ar–Ar[a]	Ar—O[a]	C3–C3[b]	C3—O[b]	C—O[c]	H—O[c]	C—C[c]	H—H[c]
σ (Å)	3.40	3.02	3.77	3.15	2.99	2.71		
ε (kcal mol^{-1})	0.238	0.246	0.206	0.272	0.254	0.068		
A, kcal mol^{-1}							88368	2861
B, $Å^{-1}$							3.60	3.74
C, kcal mol^{-1} $Å^{-6}$							583.0	32.6

[a]From Cracknell and Gubbins (1993).
[b]From Bhide and Yashonath (2002).
[c]From Bhide and Yashonath (2000).

Table 3 Experimental (Exp.) and simulated (MS) low coverage adsorption heat for the aluminophosphates series

	FD (T/1000 Å^3)	Ar MS[a]/Exp[1] (kcal/mol)	Ethane MS[b]/Exp[2] (kcal/mol)	Benzene MS[c]/Exp[2] (kcal/mol)	*o*-Xylene MS[d]/Exp[3] (kcal/mol)
$AlPO_4$-11	19.1	3.4/3.7	8.0/7.2	20.5/14.8	25.5/10.2
$AlPO_4$-5	17.3	2.8/3.0	5.8/5.9	15.3/13.0	18.0/17.6
$AlPO_4$-8	17.7	2.5/2.8	5.2/–	13.3/–	16.6/–
VPI-5	14.2	2.2/2.4	4.4/4.5	12.0/9.5	14.1/–

[1]Experimental data (Reichert et al., 1994).
[2]Experimental data (Jänchen et al., 1996).
[3]Experimental data for $AlPO_4$-5 (Chiang et al., 1991) and $AlPO_4$-11 (Cavalcante et al., 2000).
[a]MS parameters (Cracknell and Gubbins, 1993).
[b]MS parameters (Bhide and Yashonath, 2002).
[c]MS parameters (Bhide and Yashonath, 2000).
[d]This study.

We found a considerable discrepancy in $AlPO_4$-11, where the simulated adsorption heat overcomes the experimental value by 5.7 kcal/mol. For *o*-xylene, we do not have enough experimental data so we can not make a conclusion about the transferability based only on experimental data. However, Jänchen et al. (1996) showed experimentally that the increasing framework density raises the heat of adsorption. The simulated values for *o*-xylene follow this tendency reasonably; however, the experimental value is strangely much lower than the value for $AlPO_4$-5. This could be related to a possible deformation of the framework in the case of *o*-xylene in $AlPO_4$-11, which has been reported to decrease the heat of adsorption in silicalite/xylenes systems (Snurr et al., 1993a). Another possibility could be an innacuracy of the experimental value previously reported (Cavalcante et al., 2000). Other experimental tendency well reproduced in the simulations is the fact that the values for $AlPO_4$-5 are always larger than those for $AlPO_4$-8, although the framework density of $AlPO_4$-5 is smaller than the FD of $AlPO_4$-8. This happens because the free diameter of $AlPO_4$-5 is smaller than that of $AlPO_4$-8. These results show that the force fields are transferable among the members of the sieves series, what encourages us to continue with the adsorption and structural analysis calculations. In Fig. 2, we show all results of adsorption heat versus framework density in two single plots (argon and ethane in Fig. 2(A), and aromatics in Fig. 2(B)), evidencing the good force field transferability for all sieves, except for the $AlPO_4$-11 results for benzene and *o*-xylene.

3.2 Adsorption isotherms

The adsorption isotherms of xylenes in $AlPO_4$-5 were simulated at 30°C and compared with experimental data of Chiang et al. (1991). Figure 3 presents the simulated and the experimental isotherms. In the experimental isotherm the adsorbed phase concentration for *p*- and *o*-xylene reaches about 80% of the total sorption capacity still at very low pressures ($P/P_o < 0.03$). $AlPO_4$-5 adsorbs *o*-xylene selectively (approximately 50% more than *p*-xylene). The simulated isotherms agree nicely with these characteristics.

The adsorbed values in the simulated isotherms are initially larger than the experimental ones. This may happen because the real sieve would probably have imperfections (not assumed for the simulated sieve) so it would need a larger bulk phase concentration to reach saturation (Boutin et al., 1994).

The simulated heat of adsorption at low coverage for *o*-xylene in $AlPO_4$-5 (18.0 kcal/mol), as shown in Table 3, presents a similar value to the one from experimental measurements (17.6 kcal/mol), which is obvious since the force field was fitted from those data. For *p*-xylene, the simulated value was 16.8 kcal/mol, which compares relatively well to the experimental value of 15.3 kcal/mol, reported by Chiang et al. (1991). For both simulated and experimental values, we notice higher heats of adsorption for *o*-xylene, which may be related to the ortho-selectivity behavior that has been observed from the experimental isotherms.

We do not have experimental adsorption data for VPI-5 and $AlPO_4$-8. So, our isotherms are only

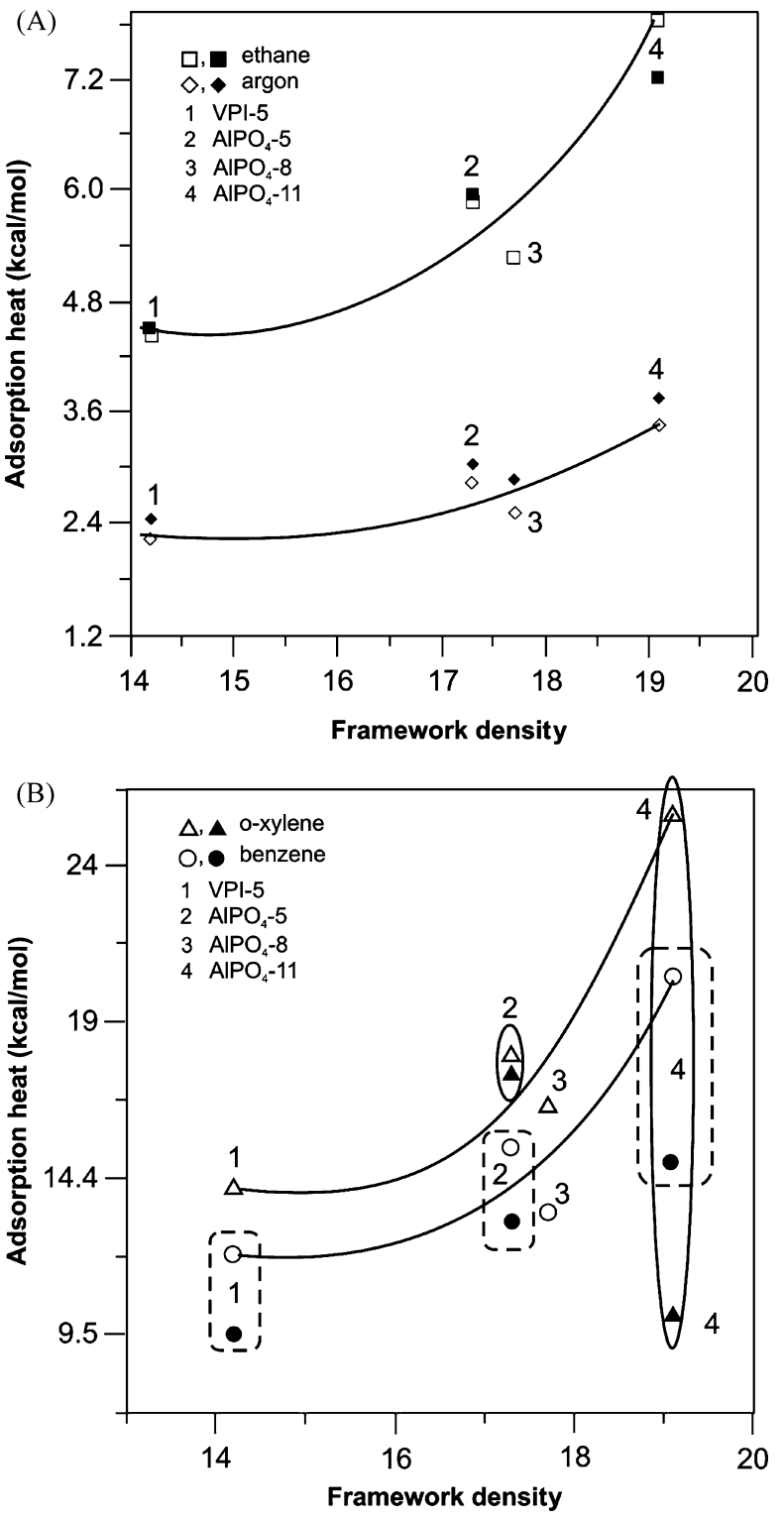

Fig. 2 Variation of heats of adsorption with framework density (Full symbols: experimental data; Blank symbols: simulation data)

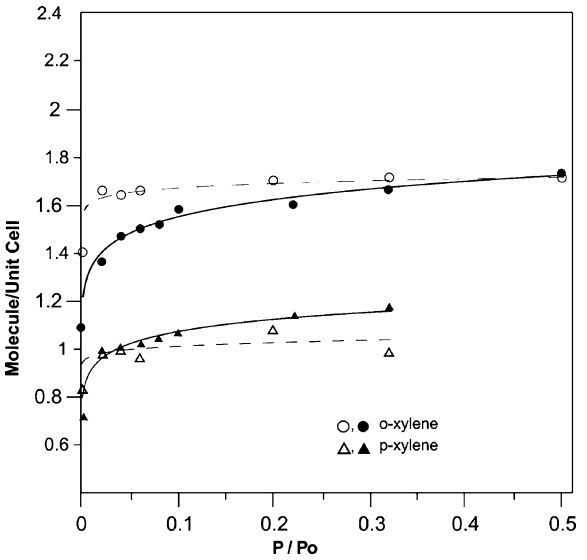

Fig. 3 Adsorption isotherms of xylenes in $AlPO_4$-5 at 30°C. Our simulation (dashed lines and open symbols); experimental data from Chiang et al. (filled lines and symbols)

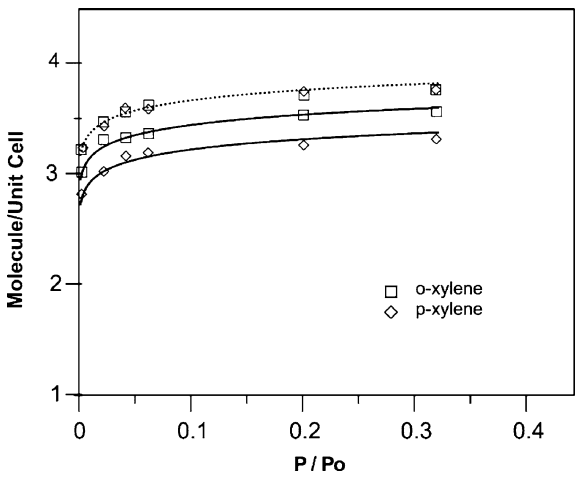

Fig. 4 Simulated adsorption isotherms of xylenes in $AlPO_4$-8 and VPI-5 at 30°C: $AlPO_4$-8 (filled lines); VPI-5 (dashed lines)

predictions in order to evaluate the ortho*o*-selectivity existence in those sieves. Figure 4 shows simulated adsorption isotherms for *o*- and *p*-xylene in VPI-5 and $AlPO_4$-8 at 30°C. $AlPO_4$-8 adsorbs approximately 14% more *o*-xylene than *p*-xylene, showing also a tendency to ortho-selectivity. In VPI-5 there is no difference between the adsorbed amounts of *o*- and *p*-xylene.

The mechanism that originates the different patterns of adsorption in these sieves will be examined based in the structural analysis.

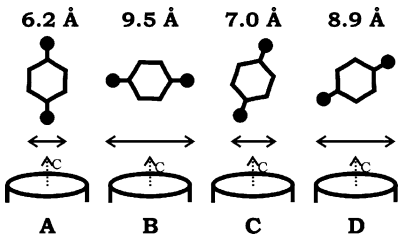

Fig. 5 The *c* axis crystallographic positioning and respective dimension of *p*-xylene configurations

3.3 Structural analysis for $AlPO_4$-8 and VPI-5

The structural analysis methodology was the same as developed in our previous work (Lucena et al., 2006). The proposal for the xylenes configurations inside the aluminophosphates pores was based on the size, in the statistics of centers of mass of the molecules, and in the xylene ring normal vector orientation. Xylene molecular sizes were estimated and several configurations were proposed for the xylenes molecules. For VPI-5 any configuration of the xylenes molecules can be admitted. For $AlPO_4$-8 the p-xylene configuration B would not be admitted into the pores (see Fig. 5).

3.3.1 $AlPO_4$-8

o-Xylene. The statistical analysis of the mass center projection of the *o*-xylene molecules on the plane (0 0 1) demonstrates that they occur in two positions (see Fig. 6(A)): 1- in a circular perimeter at the $AlPO_4$-8 pore center (marked with letter C) and 2- near the pore wall, out of the pore center. This same analysis on the plane (0 1 0) is shown in Fig. 6(B). We can make a correlation between the two projections and see that the pore center position occurs preferentially in the wide regions and the wall position in the narrow oxygen windows (positions A and B respectively in Fig. 7).

The evaluation of the angles between the perpendicular xylene ring vector and the crystallographic *c* axis shows two bands. One with low angle that corresponds to a face-to-face position of *o*-xylene (position A in Fig. 7). The other one has a high angle and is compatible with the position that the aromatic ring is almost parallel to the pore walls (position B in Fig. 7).

It is observed that the configuration that promotes ortho-selectivity in $AlPO_4$-5 also appears in $AlPO_4$-8. While in $AlPO_4$-5 practically all the molecules are in the face to face position, in $AlPO_4$-8 only 33% of the

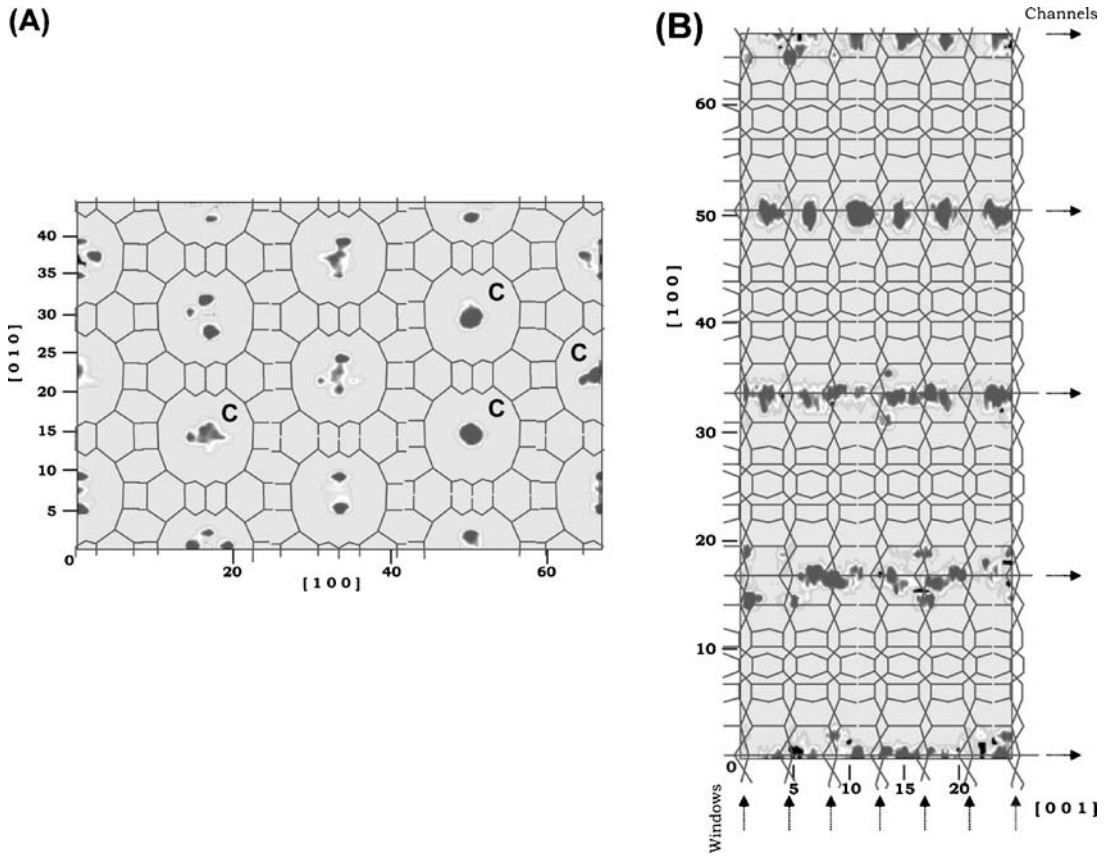

Fig. 6 View of the $3 \times 3 \times 3$ simulation cell of $AlPO_4$-8 and *o*-xylene with respective statistics of mass centers location of the success moves during simulation. (A) Projection down plane (0 0 1). Letter C marks where molecule occurs in the pore center; (B) Projection down plane (0 1 0). Dark areas are of high mass centers occurrence

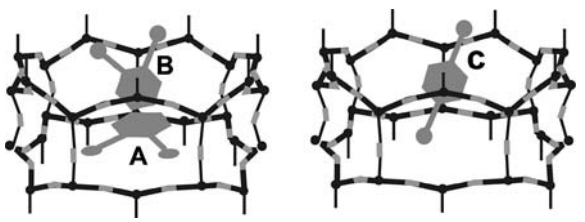

Fig. 7 Representation of *o*-xylene (A) and (B), and *p*-xylene (C) molecules adsorbed in the $AlPO_4$-8 channels at 30°C. (A) Molecules of *o*-xylene positioned face to face in wide region; (B) Molecules of *o*-xylene positioned parallel to the pore walls; (C) Molecules of *p*-xylene positioned parallel to the pore walls

o-xylene occurrences correspond to the face to face position (marked with letter C in Fig. 6(A)).

It may also be noted that the variation of the channel diameter continues to be decisive in the molecule pore configuration and determine the adsorption sites. The face to face position occurs preferentially in the wide region and the parallel position in the narrow windows position.

A typical image of the two possible positions for the *o*-xylene molecules in $AlPO_4$-8 channels is shown in Fig. 8.

p-Xylene. The statistical analysis of the mass center projection of the *p*-xylene molecules on the plane (0 0 1) demonstrates that they do not occur in the pore center, only near the pore walls (see Fig. 9(A)). This same analysis on the plane (0 1 0) confirms this observation (Fig. 9(B)). The wall position occurs preferentially in the wide regions, in which the aromatic ring can move closer to the pore surface than for the narrow window regions.

The evaluation of the angles between the perpendicular xylene ring vector and the crystallographic *c* axis shows only one high angle band. This angle band is

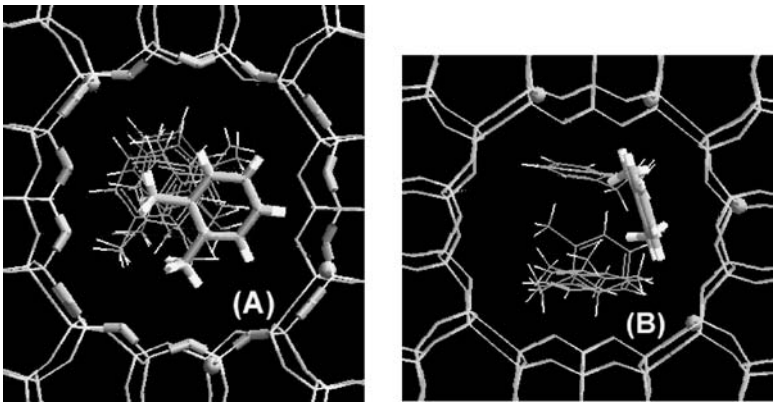

Fig. 8 Pore superior view of the *o*-xylene molecules adsorbed in $AlPO_4$-8 pores at 30°C, showing the suggested patterns. (A) Face to face; (B) Parallel position

compatible with the position that the aromatic ring is almost parallel to the pore walls (position C in Fig. 7).

The predominance of the parallel position for *p*-xylene is probably the reason of the lower adsorption loadings when compared to *o*-xylene. The variation in pores diameters and the corresponding average interaction energies with the sieve framework determine once more the ortho-selectivity tendency.

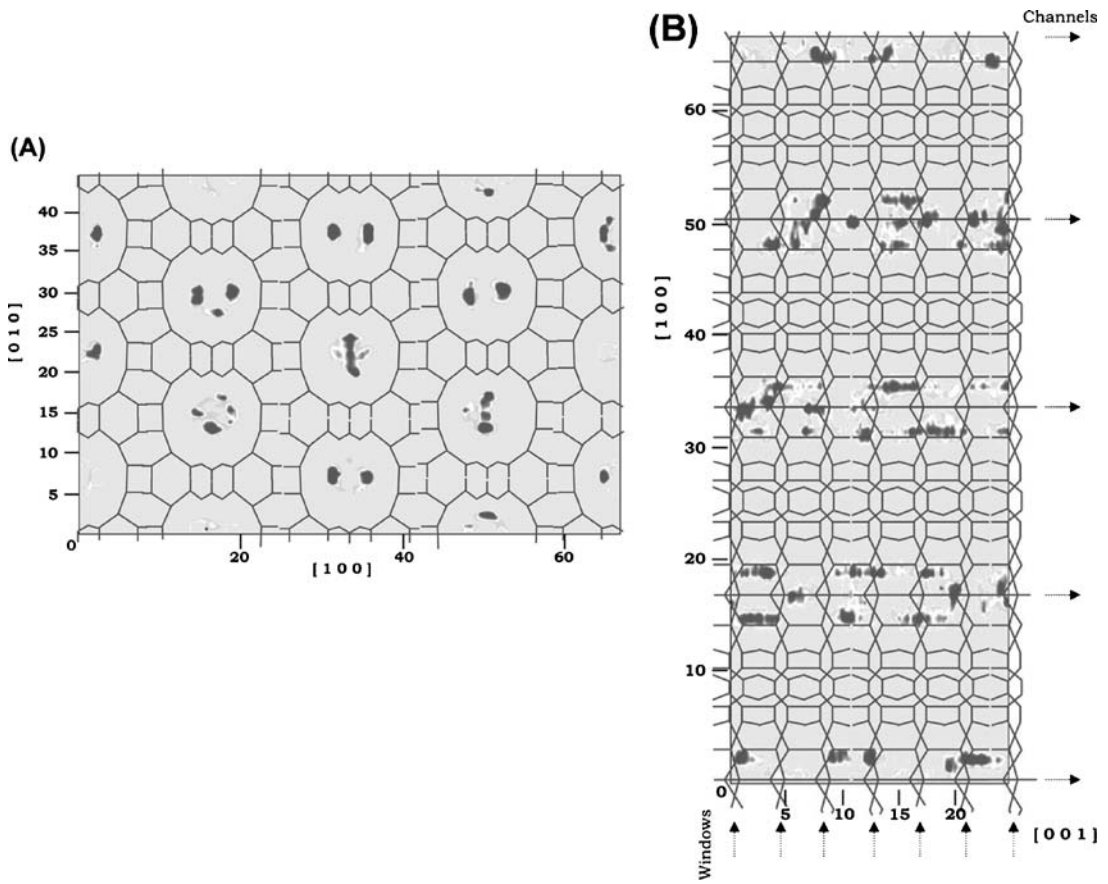

Fig. 9 View of the 3×3×3 simulation cell of $AlPO_4$-8 and *p*-xylene with respective statistics of mass centers location of the success moves during simulation. (A) Projection down plane (0 0 1); (B) Projection down plane (0 1 0). Dark areas are of high mass centers occurrence

3.3.2 VPI-5

The statistical analysis of the mass center projection of *o*-xylene and *p*-xylene molecules on the plane (0 0 1) demonstrates that they occur away from the pore centers and only near the pore walls (see Fig. 10(A)). Making a correlation with the (0 1 0) projection (see Fig. 10(B)) we can see that they occur in wide and narrow regions and it is difficult to determine an exact adsorption site. The same observation is valid to *p*-xylene and we can not notice differences between the orto or para-xylenes configurations.

The evaluation of the angles between the perpendicular xylene ring vector and the crystallographic *c*

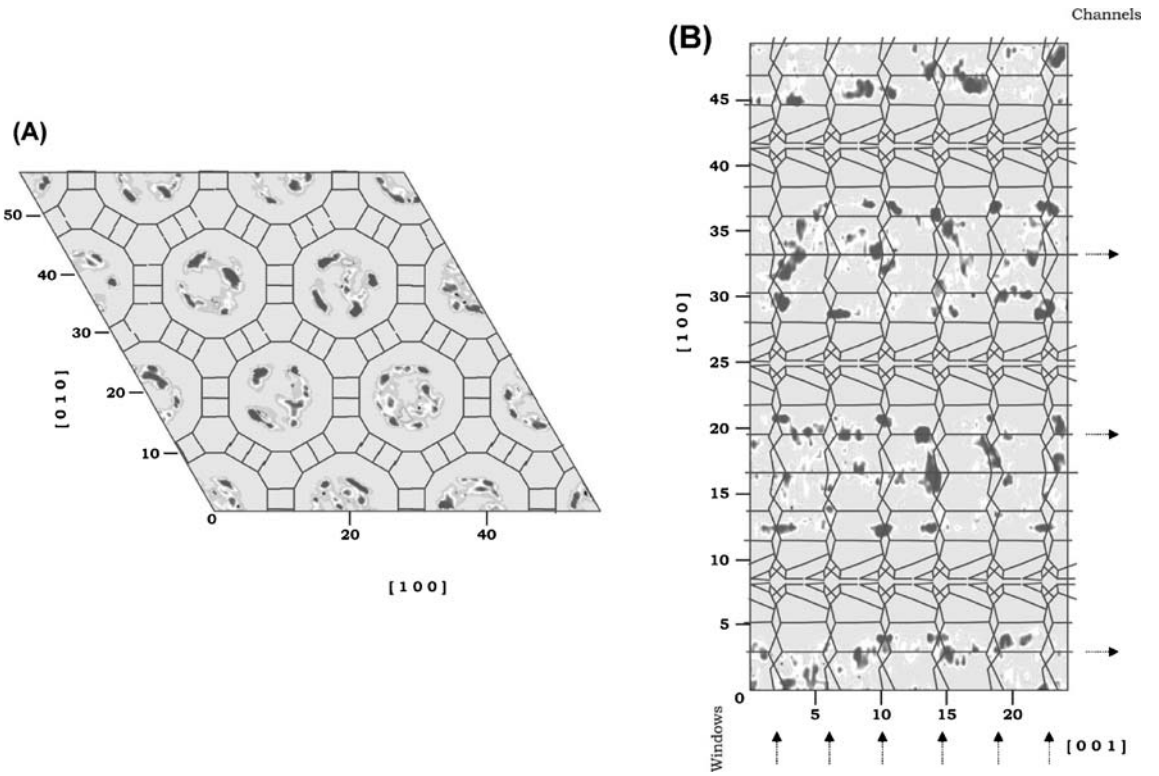

Fig. 10 View of the 3×3×3 simulation cell of VPI-5 and *o*-xylene with respective statistics of mass centers location of the success moves during simulation. (A) Projection down plane (0 0 1); (B) Projection down plane (0 1 0). Dark areas are of high mass centers occurrence

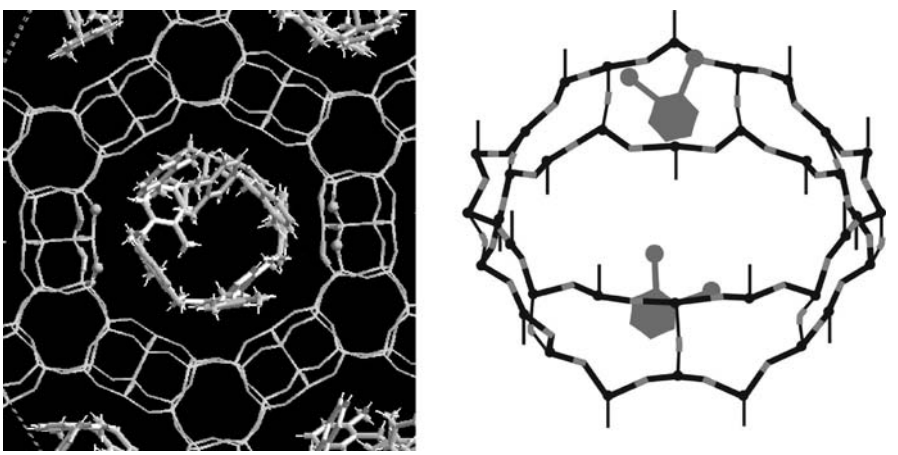

Fig. 11 Pore superior view and representation of *o*-xylene molecules adsorbed in the VPI-5 channels at 30°C. A similar picture is valid to *p*-xylene

axis shows only high angle bands for the two xylenes (aromatic ring almost parallel to the pore walls). This picture is compatible with the VPI-5 simulated adsorption isotherms that did not show any evidence of ortho-selectivity.

A typical illustration of the xylenes position in the VPI-5 pores is shown in Fig. 11.

4 Conclusions

A new force field fitted for xylenes in aluminophosphates has been presented. The force field transferability was evaluated among aluminophosphates. The transferability study showed good correlation among the several aluminophosphate sieves.

With the new force field it was possible to reevaluate the *o*-xylene and *p*-xylene/$AlPO_4$-5 isotherms and eliminate some discrepancies found in our previous work (Lucena et al., 2006) in which an approximated force field was used. Besides the fine agreement between the adsorption curves, the simulations showed the same experimental adsorption difference that confirms the ortho-selectivity evidence in those sieves. A good correlation was also obtained between experimental adsorption heat values and simulated values.

Having good aluminophosphate force fields transferability and $AlPO_4$-5 adsorption isotherms results, we extended the analysis for $AlPO_4$-8 and VPI-5. We calculated ortho- and para-xylene isotherms for those two sieves. The isotherms of $AlPO_4$-8 showed evidence of ortho-selectivity (*o*-xylene adsorbs 14% more than *p*-xylene at saturation conditions) while the VPI-5 isotherm did not show any difference in adsorbed phase concentration values.

We performed a structural analysis for the $AlPO_4$-8 and VPI-5 sieves to investigate the mechanism that generates ortho-selectivity in $AlPO_4$-8 and its absence in VPI-5. The simulations confirmed the same ortho-selectivity mechanism previously proposed (Lucena et al., 2006) and defined the adsorption sites of $AlPO_4$-8 and the absence of specific adsorption sites for VPI-5.

For $AlPO_4$-8 and VPI-5 it would not be possible to predict the configuration of the molecules only using experimental adsorption data and molecular sizes, since we have large pores and more than one molecule can adsorb in the same site. In this case, the use of the molecular simulation tools was decisive for predicting the xylenes configurations.

Acknowledgments The authors wish to acknowledge financial support for this study from CAPES, CNPq and FINEP/CTPETRO. Motivating and fruitful discussions with Prof. Randall Snurr during S.M.P. Lucena's short stay with his group at Northwestern University (Evanston, Ill) are also gratefully acknowledged.

References

Barthomeuf, D. and A. De Mallmann, "Adsorption of Aromatics in NaY and $AlPO_4$-5. Correlation with the Sorbent Properties in Separations," *Ind. Eng. Chem. Res,* **29**, 1435–1438 (1990).

Bennett, J.M., J.P. Cohen, E.M. Flanigen, J.J. Pluth, and J.V. Smith, "Crystal Structure of Tetrapropylammonium Hydroxide-Aluminum Phosphate Number 5," *ACS Symp. Ser.*, **218**, 109–118 (1983).

Bennett, J.M., J.W. Richardson, J.J. Pluth, and J.V. Smith, "Aluminophosphate Molecular Sieve AlPO4-11: Partial Refinement from Powder Data Using a Pulsed Neutron Source," *Zeolites*, **7**, 160–162 (1987).

Bhide S.Y. and S. Yashonath, "Study of Translational and Rotational Mobility and Orientational Preference of Ethane in One-Dimensional Channels," *J. Phys. Chem. A,* **106**, 7130–7137 (2002).

Bhide, S.Y. and S. Yashonath, "Structure and Dynamics of Benzene in One-Dimensional Channels," *J. Phys. Chem. B*, **104**, 11977–11986 (2000).

Boutin, A., R.J.-M. Pellenq, and D. Nicholson, "Molecular Simulations of the Stepped Adsorption Isotherm of Methane in $AlPO_4$-5," *Chem. Phys. Letters*, **219**, 484–490 (1994).

Cavalcante Jr., C.L., D.C.S. Azevedo, I.G. Souza, A.C.M. Silva, O.L.S. Alsina, V.E. Lima, and A.S. Araujo, "Sorption and Diffusion of *p*-Xylene and *o*-Xylene in Aluminophosphate Molecular Sieve $AlPO_4$-11," *Adsorption*, **6**, 53–59 (2000).

Chiang, A.S.T., C.K. Lee, and Z.H. Chang, "Adsorption and Diffusion of Aromatics in $AlPO_4$-5," *Zeolites*, **11**, 380–386 (1991).

Clark L.A. and R.Q. Snurr, "Adsorption Isotherm Sensitivity to Small Changes in Zeolite Structure," *Chem. Phys. Letters*, **308**, 155–159 (1999).

Cracknell, R.F. and K.E. Gubbins, "Molecular Simulation of Adsorption and Diffusion in VPI-5 and Other Aluminophosphates," *Langmuir*, **9**, 824–830 (1993).

Cracknell, R.F. and K.E. Gubbins, "A Monte Carlo Study of Methane Adsorption in Aluminophosphates and Porous Carbons," *J. Molec. Liquids*, **54**, 261–271 (1992).

Demontis, J.P., S. Yashonath, and M.L. Klein, "Localization and Mobility of Benzene in Sodium-Y Zeolite by Molecular Dynamics Calculations," *J. Phys. Chem.*, **93**, 5016–5019 (1989).

Dessau, R.M., J.L. Schlenker, and J.B. Higgins, "Framework Topology of $AlPO_4$-8: The First 14-Ring Molecular Sieve," *Zeolites*, **10**, 522–524 (1990).

Eder, F. and J.A. Lercher, "Alkane Sorption on Siliceous and Aluminophosphate Molecular Sieves. A Comparative Study," *J. Phys. Chem.*, **100**, 16460–16462 (1996).

Frenkel D. and B. Smit, *Understanding Molecular Simulation*, Academic Press, New York, 2002.

Jänchen, J., H. Stach, L. Uytterhoeven, and W.J. Mortier, "Influence of the Framework Density and Effective Electronegativity of Silica and Aluminophosphate Molecular Sieves on the Heat of Adsorption od Nonpolar Molecules," *J. Phys. Chem.*, **100**, 12489–12493 (1996).

Jorgensen, W.L., E.R. Laird, T.B. Nguyen, and J. Tirado-Rives, "Monte Carlo Simulations of Pure Liquid Substituted Benzenes with OPLS Potential Functions," *J. Comp. Chem.*, **14**, 206–215 (1993).

Kiselev, A.V., A.A. Lopatkin, and A.A. Shulga, "Molecular Statistical Calculation of Gas Adsorption by Silicalite," *Zeolites*, **5**, 261–267 (1985).

Lachet, V., A. Boutin, B. Tavitian, and A.H. Fuchs, "Computational Study of *p*-Xylene/*m*-Xylene Mixtures Adsorbed in NaY Zeolite," *J Phys. Chem. B*, **102**, 9224–9233 (1998).

Lachet, V., A. Boutin, B. Tavitian, and A.H. Fuchs, "Molecular Simulation of *p*-Xilene and *m*-Xylene Adsorption in *Y* Zeolites. Single Components and Binary Mixtures Study," *Langmuir*, **15**, 8678–8685 (1999).

Lucena, S.M.P., J.A.F.R. Pereira, and C.L. Cavalcante Jr., "Structural Analysis and Adsorption Sites of Xylenes in $AlPO_4$-5 and $AlPO_4$-11 Using Molecular Simulation," *Micro. Meso. Materials*, **88**, 135–144 (2006).

McCullen S.B., P.T. Reischman, and D.H. Olson, "Hexane and Benzene Adsorption by Aluminophosphates and SSZ-24: The Effect of Pore Size and Molecular Sieve Composition," *Zeolites*, **13**, 640–644 (1993).

McCusker, L.B., Ch. Baerlocher, E. Jahn, and M. Bülow, "The Triple Helix Inside the Large-Pore Aluminophosphate Molecular Sieve VPI-5," *Zeolites*, **11**, 308–313 (1991).

Reichert, H., W. Schmidt, Y. Grillet, P. Llewellyn, J. Rouquerol, and K. Unger, "Investigation on the Adsorption of N2, Ar, CO and CH_4 on Aluminophopsphates," *Stud. Surf. Sci. Catal*., **87**, 517–524 (1994).

Snurr, R.Q., A.T. Bell, and D.N. Theodorou, "Prediction of Adsorption of Aromatic Hydrocarbons from Grand Canonical Monte Carlo Simulations with Biased Insertions," *J. Phys. Chem.*, **97**, 13742–13752 (1993a).

Snurr, R.Q., A.T. Bell, and D.N. Theodorou, "Molecular Simulations of Low Occupancy Adsorption of Aromatics in Silicalite," *Proceedings from the Ninth International Zeolite Conference*, **II**, 71–78, (1993b).

Sorption, *Invoked from Cerius2 v. 4.6*, Accelrys Inc, San Diego, 2001.

Sun, H., S.J. Mumby, J.R. Maple, and A.T. Hagler, "An Ab Initio CFF93 All-atom Force Field for Polycarbonates," *J. Amer. Chem. Soc.*, **116**, 2978–2987 (1994).

Wilson, S.T., M.L. Brent, C.A. Messina, T.R. Cannan, and E.M. Flanigen, "Aluminophosphate Molecular Sieves: A New Class of Microporous Crystalline Inorganic. Solids," *J. Am. Chem. Soc.*, **104**, 1146–1147 (1982).